

International Conference on Space Optics—ICSO 2022

Dubrovnik, Croatia

3–7 October 2022

Edited by Kyriaki Minoglou, Nikos Karafolas, and Bruno Cugny,



In flight stray light reduction for the Solar Orbiter/Metis coronagraph



In flight stray light reduction for the Solar Orbiter/Metis coronagraph

Federico Landini^a, Marco Romoli^b, Gianalfredo Nicolini^a, Fabio Frassetto^c, Roberto Susino^a, Lucia Abbo^a, Vincenzo Andretta^d, Aleksandr Burtovoi^e, Chiara Casini^{c,o}, Paolo Chioetto^{c,o}, Alain J. Corso^c, Vania Da Deppo^c, Yara De Leo^{f,g}, Michele Fabi^h, Silvano Fineschi^a, Federica Frassati^a, Catia Grimani^h, Petr Heinzlⁱ, Giovanna Jerse^j, Alessandro Liberatore^k, Giampiero Naletto^l, Maurizio Pancrazzi^a, Giuliana Russano^d, Clementina Sasso^d, Daniele Spadaro^f, Marco Stangalini^m, Daniele Telloni^a, Luca Teriaca^f, Michela Uslenghiⁿ, Cosimo A. Volpicelli^a, and Paola Zuppella^c

^aINAF - Osservatorio Astrofisico di Torino, Via Osservatorio 20, Pino Torinese, Italy

^bDipartimento di Fisica e Astronomia, Università degli Studi di Firenze, Via Sansone 1, Sesto Fiorentino, Italy

^cCNR - Institute for Photonics and Nanotechnologies, Via Trasea 7, Padova, Italy

^dINAF - Osservatorio Astronomico di Capodimonte, Salita Moiariello 16, Napoli, Italy

^eINAF - Osservatorio Astrofisico di Arcetri, Largo Enrico Fermi 5, 50125, Firenze, Italy

^fINAF - Osservatorio Astrofisico di Catania, Via S.Sofia 78, Catania, Italy

^gMax Planck Institute for Solar System Research, Justus-von-Liebig-Weg 3, Göttingen, Germany

^hUniversità degli Studi di Urbino Carlo Bo, Via Santa Chiara 27, Urbino, Italy

ⁱAstronomical Institute of the Czech Academy of Sciences, Prague, Czech Republic

^jINAF, Osservatorio Astronomico di Trieste, Via G.B. Tiepolo 11, Trieste, Italy

^kJet Propulsion Laboratory, California Institute of Technology, Pasadena, CA 91109, USA

^lDipartimento di Fisica e Astronomia, Università di Padova, Via Marzolo 8, Padova, Italy

^mItalian Space Agency (ASI), Via del Politecnico, Roma, Italy

ⁿINAF - Istituto di Astrofisica Spaziale e Fisica Cosmica, Via Alfonso Corti 12, Milano, Italy

^oCISAS, Centro di Ateneo di Studi e Attività Spaziali “Giuseppe Colombo”, Via Venezia 15, 35131 Padova, Italy

ABSTRACT

After the 10th February 2020 launch (04:03 UTC), Solar Orbiter has recently begun its Nominal Mission Phase and is collecting imaging data as never seen before due to its peculiar orbit. The Metis coronagraph produces maps of the linearly polarized visible light corona in the wavelength band 580-640 nm and UV maps in the Lyman alpha H I 121.6 nm line. Metis is a coronagraph characterized by an innovative external occultation system that has a twofold function: reduce the thermal load and remove the diffraction due to the external occulter support. The positions of the entrance pupil (which is called Inverted External Occulter, IEO) and of the actual occulter are switched so that the pupil is the surface facing the solar disk and the occultation is performed by a spherical mirror, M0. M0 is positioned 800 mm behind IEO and reflects the disk light back through the IEO aperture. An Internal Occulter (IO) is conjugated to the IEO with respect to the primary mirror. IO is mounted on a motorized 2-axis stage that allows to perform in-flight fine adjustments to its position. During the on-ground calibration campaign the contribution of the stray light due to the diffraction from the IEO and scattering off the optics was measured. The measurement was carried out by using the OPSys facility in

Further author information: (Send correspondence to F.L.)

F.L.: E-mail: federico.landini@inaf.it, Telephone: +39 (0)55 275 5221

Torino (Italy), which is equipped with a clean environment and a source that simulates the solar disk divergence. A stray light measurement in flight is not trivial due to the presence of the solar corona. Nevertheless, an IO position optimization campaign has been conducted in order to reduce the stray light. A procedure was developed in order to minimize the stray light level on the instrument focal plane. This contribution reports on the procedure and on the results.

Keywords: Stray light, solar coronagraph, Solar Orbiter, Motorized parts in flight, Performance evaluation, Data analysis

1. INTRODUCTION

Metis¹ is the coronagraph on-board Solar Orbiter,² successfully launched on February 10th, 2020. The spacecraft and its payload have entered its nominal mission phase at the beginning of December 2021, after a long cruise phase during which the instruments completed their characterization and started to perform the first scientific observations.³ On March 25th, 2022, Solar Orbiter approached its first close-up perihelion at 0.32 UA, which allowed its remote sensing instruments to deliver images with unprecedented spatial details. Measurements at first perihelion have shown no evident presence of stray light which confirms the performance of Metis. The scope of this paper is to summarize the work that has been performed in flight in order to improve Metis' stray light reduction performance from the first light observations⁴ to the current brilliant status.

Some details on the optical design and on the occultation system are given in sections 1.1 and 1.2. A thorough summary of the method that was used to reduce stray light in flight is presented in section 2 and an evaluation of the results is given in section 3.

1.1 Metis optical design

Metis coronagraph is designed⁵ to image the solar corona in an annular field of view (FOV) centered (in nominal flight conditions) on the solar disk center and covering the range from 1.6° to 2.9°. Metis is an externally occulted coronagraph with a novel inverted optical configuration (figure 1) that takes images in the broadband linearly polarized visible light (580-640 nm, VL channel) and, for the first time simultaneously over the entire field of view, in the narrow band H I Ly- α at 121.6 nm (UV channel). The instrument consists of a single on-axis gregorian telescope with the UV and the VL channel, that are separated by an interference filter tuned at 121.6 nm that reflects the visible light and transmits the UV light. Metis adopts an innovative occultation solution, which

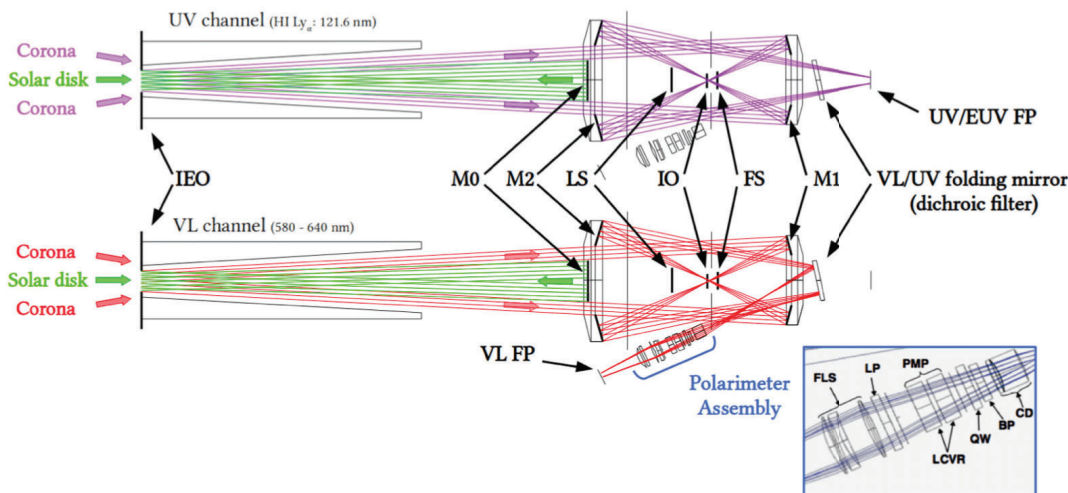


Figure 1: Metis ray trace for the UV and VL channels with a zoom on the VL polarimeter assembly.⁴

is based on switching positions between entrance aperture and occulter. The entrance aperture is called inverted

external occulter, IEO, and consists of a circular opening which is directly exposed to the direct solar disk light. The M0 spherical mirror, positioned 800 mm behind the IEO, rejects the solar disk by focusing its image on the IEO itself. The IEO diaphragm is actually the top aperture of a truncated cone,^{6,7} whose internal surface prevents light diffracted by the top aperture from reaching the instrument telescope. In addition, the image of the IEO edge produced by the primary mirror, M1, is blocked by a position adjustable internal occulter, IO, described in detail in section 1.2.

A field stop (FS) is located at the primary focal plane, while a Lyot Stop is conjugated to the M0 mirror with respect to M1. The FS is limiting the outer field of view. The LS is blocking the light diffracted by the M0 edge and imaged by M1. The secondary mirror M2 is then forming the coronal image onto the UV focal plane. In front of the UV detector, an interference filter is reflecting the visible light off-axis towards the polarimetric assembly of the VL channel. The visible solar corona is then processed by the polarimeter⁵ and imaged onto the VL detector.

Metis design allows also to operate the coronagraph when the spacecraft is off-pointed with respect to the center of the Sun, permitting a limited operability of the instrument during Solar Orbiter active region pointing and/or tracking, that depends on the heliospheric distance of Solar Orbiter (limb pointing above 0.5 AU distance is possible¹).

1.2 The Internal Occulter

Metis internal occulter is a circular aperture with a diameter of 5.0 mm, conjugated to the IEO with respect to the primary mirror M1. It is designed in order to block the light diffracted by the IEO edge and imaged by M1. It is a critical element, a potential single point of failure for the whole instrument. Therefore it has been decided to allow in flight modifications of its alignment position perpendicularly to the optical axis, by means of a motorized 2-axis stage.

The motorized stage is composed by two stepper motors with a step size of about 6 μm . The motors orientations are perpendicular and are conventionally named X and Y. Each motor can be operated in the two opposite directions, which we conventionally consider “positive” and “negative”. Motors can be operated in relative mode only, thus the “zero” reference position can vary and is defined as the IO position at the Metis turn-on (each time the system is turned off, the telemetry status of the IO position is reset).

Due to the mechanical configuration shown in figure 2 (a), the movement of a single motor affects the position of the other one. Therefore moving only one axis from one end to the other would result in a not linear movement inducing stress on the fixed pivot. Such operations are therefore avoided, preferring alternate small movements of each motor. Each motor movement affects the displacement of the circular dark shadow on the visible light image, as shown in figure 2 (b). A first adjustment of the IO position through the motors was needed during the on-ground calibration phase, as described in Romoli et al. (2021).⁴ After launch further modifications were performed, as described in the next section.

2. IN FLIGHT STRAY LIGHT REDUCTION

Metis underwent three successive stages for optimizing its stray light reduction performance. The first one was the investigation on the huge stray light level found during the first light.⁴ The investigation led to the conclusion that the main responsible for the stray light level was the misalignment of the IO. Two successive commissioning stages were dedicated to the coarse and fine tuning of the IO position to the aim of minimizing the stray light.

2.1 IO position coarse adjustment

After Metis first light, a coarse optimization has been performed by adjusting the IO position with the procedure described in a different paper⁴ that we briefly summarize hereafter.

In principle, a stray light pattern could be due to an off-pointing of Metis with respect to the solar center, a misalignment of the IO or a combination of the two effects. In order to disentangle the effects we adopted the procedure depicted in figure 3. The edge of the IEO is represented by the two red dots A and B in the sketch section of figure 3. In case everything is aligned, as shown in figure 3 (a), the image of A and B is formed on the IO plane, in a and b, respectively. If IO is properly positioned and Metis is off-pointed, then A and B are still

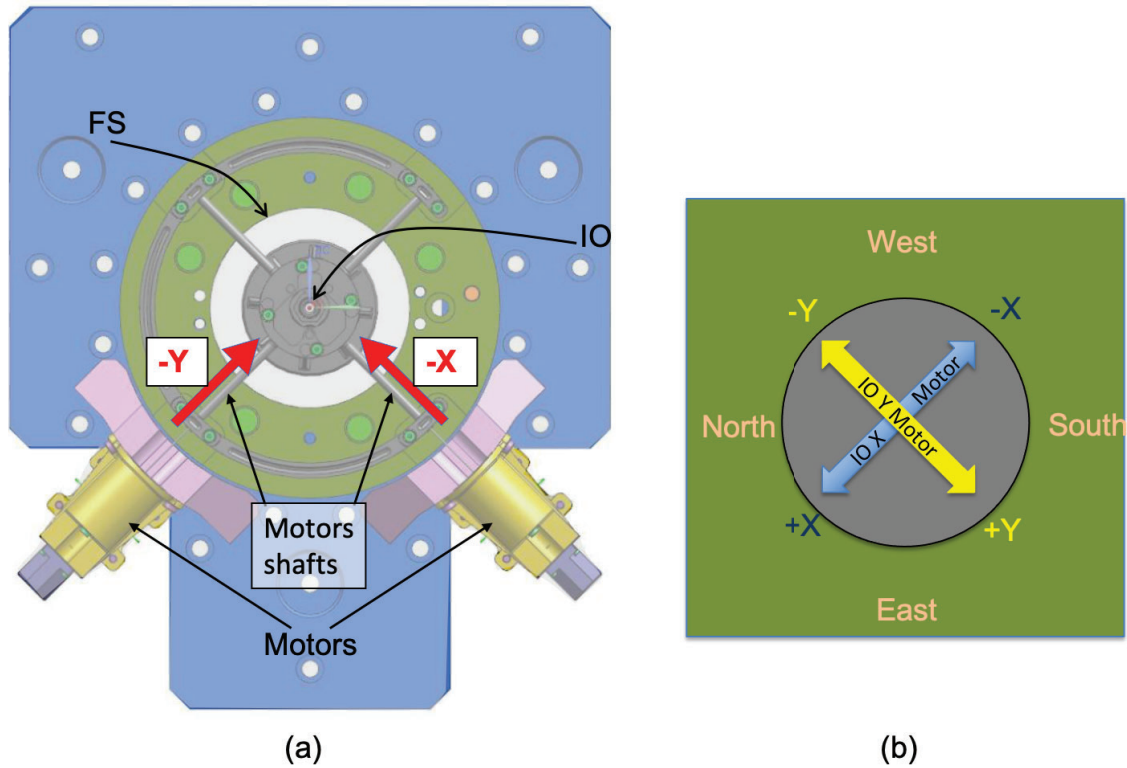


Figure 2: (a) 3D CAD of the IO assembly as seen from the secondary mirror M2. (b) Effects of IO movements on the visible light camera FOV.

imaged in a and b, while an excess of solar signal is seen on the focal plane in correspondence of the orange dot, as shown in figure 3 (b). In case Metis is pointed at the solar disk center and IO is misaligned, then a portion of the diffraction generated by the IEO edge is not correctly blocked by the IO. In the example of figure 3 (c), the red dot corresponding to the image of A is not blocked by IO and its image is propagated by M2 down to the focal plane. In figure 3 (d) the most general case is presented, with both Metis off-pointed and IO misaligned. Two acquisitions are performed, I_0 in the nominal spacecraft position and I_{180} with a spacecraft roll of 180 degrees. Please be aware that in figure figure 3 the Metis detector is marked by a flag on one side in order to easily infer its orientation after the roll. We can reasonably assume that each image, after being cleaned for the background and instrumental vignetting, is made by the corona and stray light signals summed together:

$$\begin{cases} I_0 = C_0 + S_0 \\ I_{180} = C_{180} + S_{180} \end{cases} \quad (1)$$

where C is the coronal signal and S is the stray light. The subscript indicates the roll angle. Images are acquired in the same instrumental conditions before and after a S/C roll of 180° in order to disentangle the alignment effects.

During analysis, a rotation of 180° with respect to the S/C pointing center is applied to the image acquired with roll= 180° , in order to align the coronal frame of reference with that of the image acquired with roll= 0° :

$$I_{180}^R = C_{180}^R + S_{180}^R \quad (2)$$

In the hypothesis of Metis perfectly aligned with the S/C, the S/C pointing at the Sun center both before and

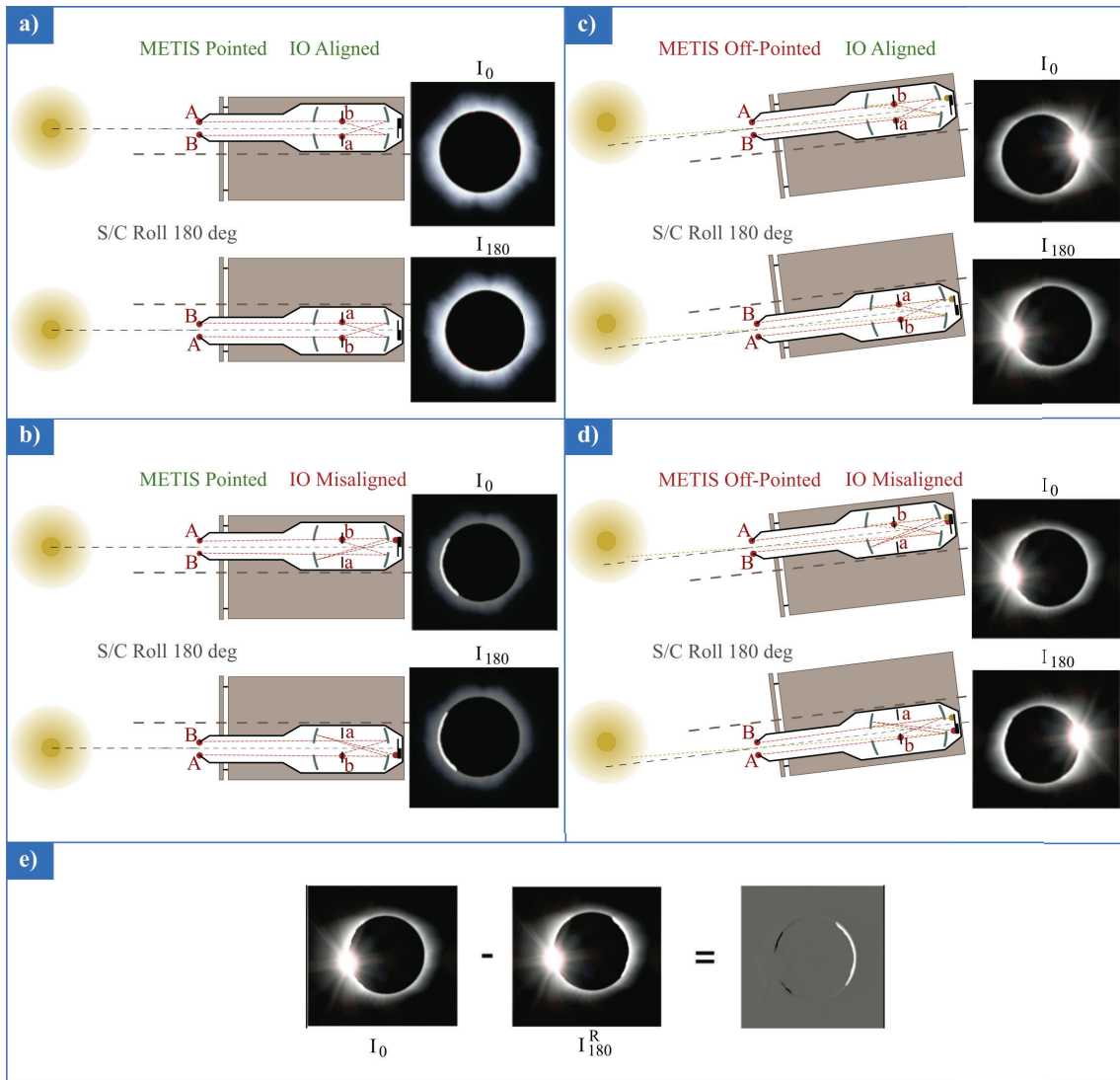


Figure 3: Method to disentangle the misalignment effects on Metis focal plane (see text for description).

after the roll and a negligible variation of the corona during the roll maneuver, we can write:

$$\begin{cases} S_{180} = S_0 \\ C_{180}^R = C_0 \end{cases} \quad (3)$$

Thus by subtracting the two images we obtain:

$$I_0 - I_{180}^R = C_0 + S_0 - (C_{180}^R + S_{180}^R) = S_0 - S_{180}^R \quad (4)$$

that is a difference of stray light maps, as shown in the sketch example of figure 3 (e). It is worth noticing that the second hypothesis of equation (3) is as much valid as the time range between the two acquisitions is short and the solar activity is far from a maximum.

In case of no S/C attitude errors and the whole alignment mismatch is originated by a bad positioning of IO, the stray light difference map will be made of negative and positive areas, symmetric with respect to the center

of the image.

The data analysis to identify an optimized IO position has been performed both qualitatively and quantitatively.

- Qualitative analysis: a careful visual inspection has been performed by comparing images acquired at different IO positions.
- Quantitative analysis: the average of the signal has been measured for each IO position over a set of ROIs (Regions Of Interest). ROIs are drawn as circular sectors around the IO edge position on the stray light difference maps and oriented along the IO motor directions, as shown in figure 4. An exception is the red ROI shown in figure 4 (b), which is used to sample the stray light behaviour with the IO movement in a region far from the IO edge.

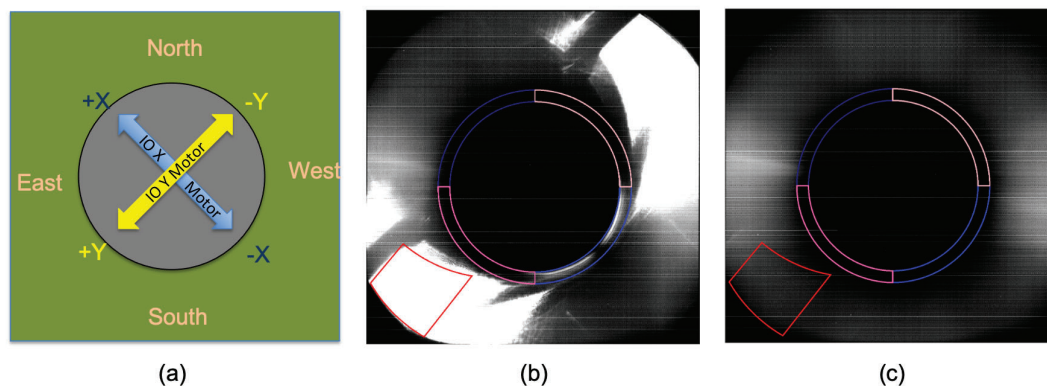


Figure 4: (a) Sketch of the Metis visible light frame with emphasis on the IO motor directions. The cardinal points on the Sun are shown as well. (b) ROIs drawn over one of the raw coronal images before IO coarse optimization. (c) Same as (b), after IO coarse optimization.

The procedure to align IO is quantitatively based upon balancing the “positive” and “negative” areas in the difference image. The result shall be in agreement as much as possible with the outcome of the qualitative analysis.

The result of the coarse optimization process is a movement along the X negative direction of ~ 0.18 mm. The raw image after the coarse optimization is shown in figure 4 (c). Some coronal features can be easily recognized.

2.2 IO position fine tuning

After the coarse IO position optimization, the solar corona could be acquired by Metis, even though a faint stray light pattern could still be perceived superimposed to the coronal signal. The coarse optimization had been performed at a heliocentric distance of about 0.6 AU while the mission perihelion had to be below 0.3 AU. Below 0.3 AU the solar disk angular dimension is doubled with respect to 0.6 AU. Without a further IO optimization, stray light conditions would have worsened in correspondence of the most interesting phases of the mission. It was then decided to perform an additional IO optimization. The fine tuning was performed at a heliocentric distance of 0.5 AU. Stray light conditions due to the distance from the Sun are not so worse with respect to the coarse optimization that the same method described in section 2.1 would give a different result. A refined procedure was developed.

The new approach is to set up a method for the definition of the ROIs linked to the areas of the images where stray light is more evident, in order to have an affordable ROIs set over which the statistical analysis can be performed.

A study was performed in order to identify the image portions with the highest variability as a function of the IO position. ROIs were then defined over those portions. The stray light difference maps (one for each IO position) were packed into data cubes, a data cube for each motor movement direction. For each pixel, the standard deviation was computed through the cube layers, as sketched in figure 5. The result, for each motor

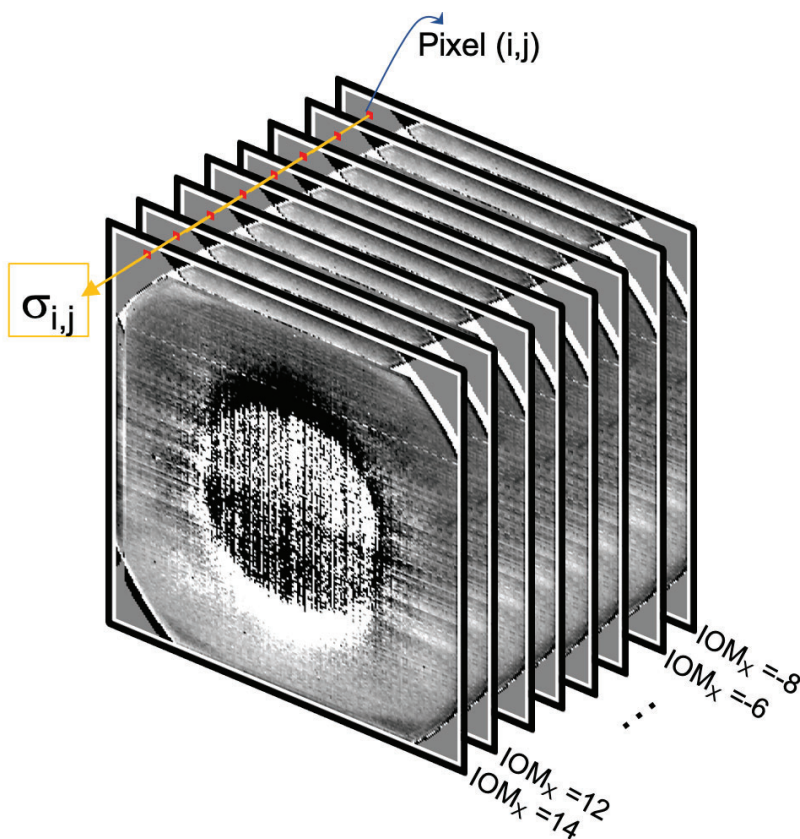


Figure 5: Sketch of the cube of layers used to compute a standard deviation map.

movement direction, is a standard deviation map, which emphasizes the areas of the stray light difference maps that underwent the highest signal variation with the motor movements. The two maps are shown in figure 6. It is quite evident from figure 6 (b) that there is almost no variation along the X movement direction, which is perpendicular to the Y movement direction for which the standard deviation was calculated. This can be taken as a confirmation of the goodness of the calculation. The same effect is also visible in the perpendicular direction in figure 6 (a), with some less evidence due to stray light patterns overlapping the axis symmetric black feature along the Y direction movement.

A further feature is also evident from the maps of figure 6: a frame is visible on top of the maps. This is due to the rotation of 180° and successive subtraction as shown by equation (4). In fact, the image pixel corresponding to the spacecraft pointing at the center of the Sun is not corresponding to the center of the frame of the Metis visible light camera and to the pixel that identifies the center of the shadow of the internal occulter. After the 180° rotation, the consequence is a shift in the rotated image with respect to the not rotated one.

Finally, it is worth noticing that Mercury can be easily spotted in the standard deviation maps, being represented by the rapidly moving shiny dot on the left side of the maps at the level of the solar equator.

The two standard deviation maps are then used for defining the ROIs, as shown in figure 7. The resulting averages in the 4 ROIs for the IO movements along the X direction are shown in the plot of figure 8 as a function of the IO position. The curve color identifies the ROIs with reference to figure 7 (a). It is worth to notice that the 0 IO position corresponds to the position defined at the end of the coarse optimization (section 2.1).

The behaviour of the red-orange curves and of the two magenta ones is in agreement and suggests an optimized position in $X = -6$ steps $\sim -36 \mu\text{m}$ at least.

The resulting averages in the 2 ROIs for the IO movements along the Y direction are shown in the plot of figure 9

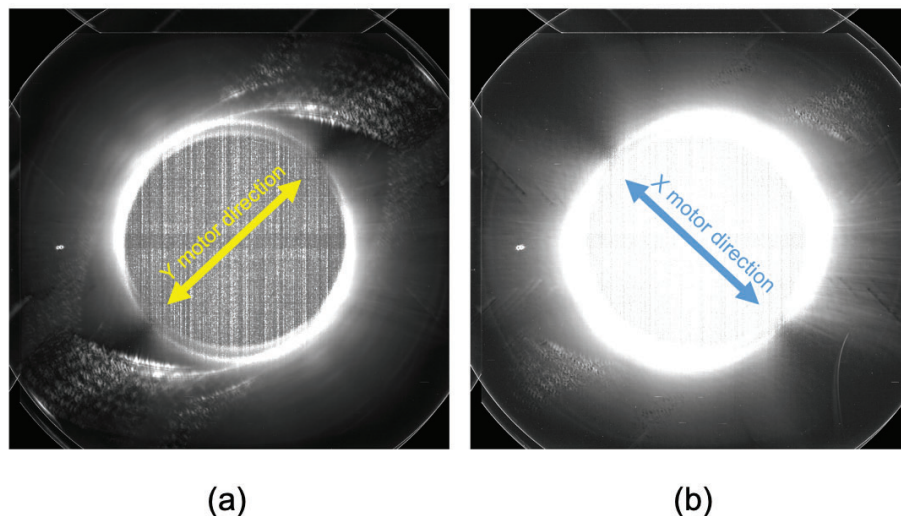


Figure 6: Standard deviation maps calculated over stray light difference maps cubes. (a) Standard deviation map for X movements. (b) Standard deviation map for Y movement.

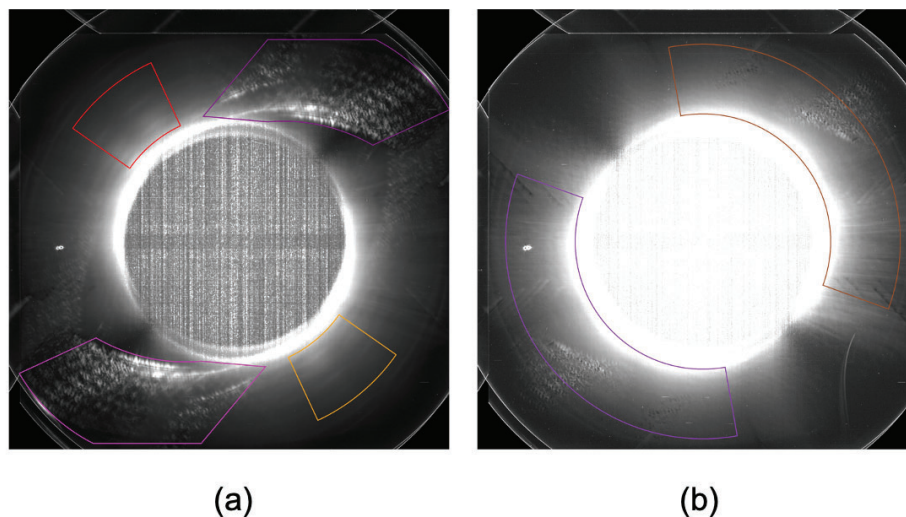


Figure 7: ROIs for qualitative evaluation of stray light variation with the IO movements, drawn on the basis of the most intense areas of the standard deviation maps (see figure 6). (a) X direction. (b) Y direction.

as a function of the IO position. The curve color identifies the ROIs with reference to figure 7 (b). The behaviour of the curves defines an optimized position in $Y = +4$ steps $\sim -24 \mu\text{m}$.

3. IMPROVEMENT EVALUATION

In this section we describe how the improvement due to the IO fine tuning was evaluated in terms of stray light reduction.

The coarse optimization (see section 2.1) was performed on May 15th, 2020, during the instrument commissioning phase, with Solar Orbiter at about 0.6 AU from the Sun. The solar activity in the first half of 2020 was still low, being close enough to a solar minimum. The IO fine adjustment (see section 2.2) was performed on February

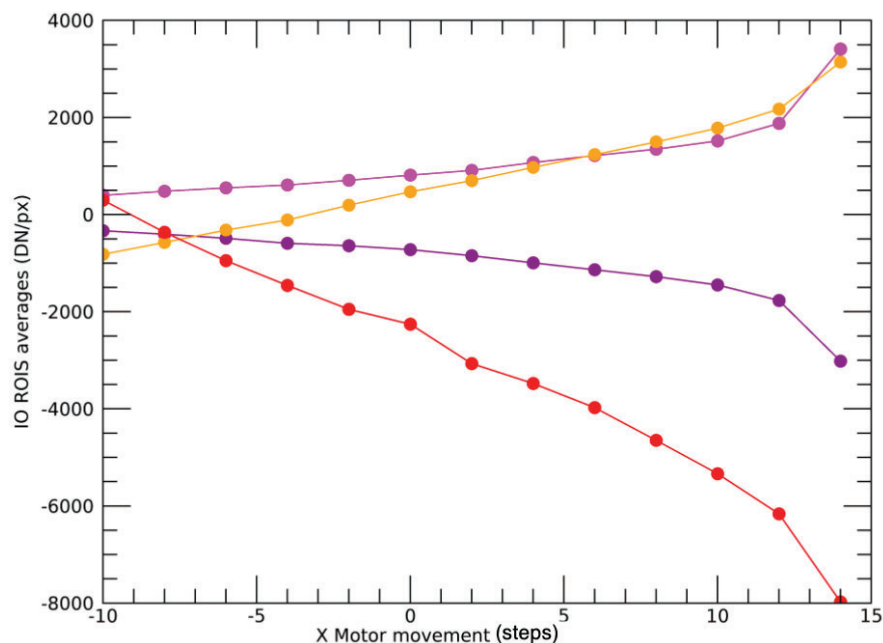


Figure 8: Stray light difference averages over the ROIs defined by figure 7 (a) as a function of the IO position along the X direction. Curve colors correspond to figure 7 (a) ROIs colors.

18, 2021, when Solar Orbiter was at a heliocentric distance of about 0.5 AU and the Sun was evolving towards a maximum of activity. This means that the corona may rapidly change and the second hypothesis of equation (3) may not be valid for the entire image. In the improvement evaluation we excluded image portions where corona was significantly changing before and after the 180° roll.

We created stray light difference maps with acquisitions taken just before (February 18, 2021) and a few days after (February 23, 2021) the IO fine tuning. The stray light difference map before the IO fine tuning is shown in figure 10 (a), the map after the tuning is shown in figure 10 (b). A percent variation is also calculated by taking the ratio of the difference of the two maps and the map before the IO fine tuning: it is useful in order to identify portions of the image with high variation of the solar corona, which are not safe to use in the comparison to evaluate the stray light reduction improvement. The percent variation map is shown in figure 10 (c). The same series of circular sectors spaced by 22.5° and centered on the IO center has been defined on the two difference maps. A representative radial profile is calculated for each sector by averaging over the 22.5° angle all profiles, with a spacing of about 10 arcsec (corresponding to the Metis angular resolution). The series of circular sectors are over-imposed on the percent variation map in figure 10 (c). The sectors between the blue and the black radial segment (both those with solid and dashed line styles) shall not be included in the comparison between post- and pre- IO fine tuning.

The ratios of averaged radial profiles computed on the stray light difference map after the tuning and before the tuning are shown in figure 11. Colors identify the sector defined by the radial segment shown in figure 10 (c): as an example, the red solid line curve in figure 11 represents the average taken over all radial profiles between the solid red and the solid black radial segments in figure 10 (c). All the curves, except for those excluded for a high variation of the solar corona, show an improvement of stray light reduction between 5% and 40% over the whole FOV. The variability depends on the portion of the image that is considered, which is differently affected by the IO position variation.

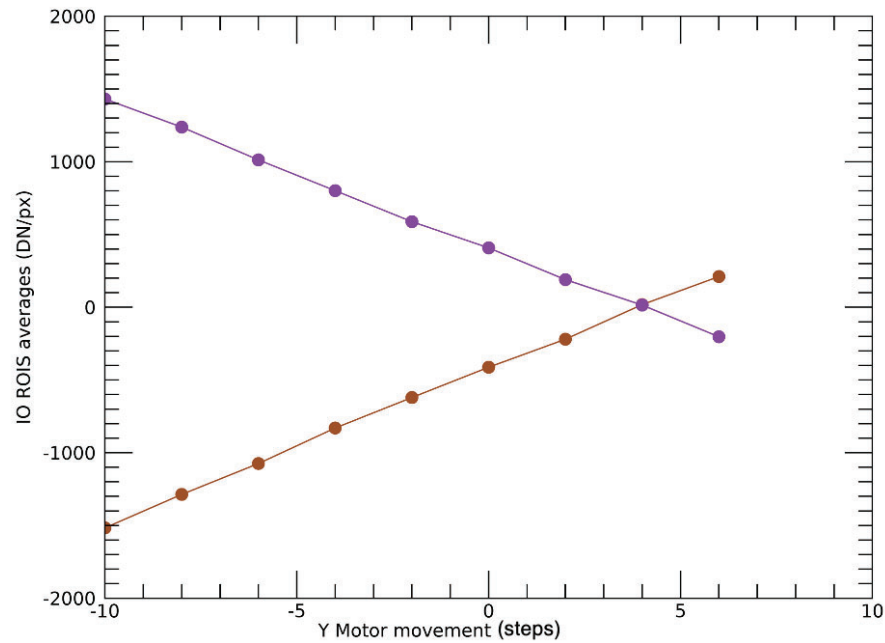


Figure 9: Stray light difference averages over the ROIs defined by figure 7 (b) as a function of the IO position along the Y direction. Curve colors correspond to figure 7 (b) ROIs colors.

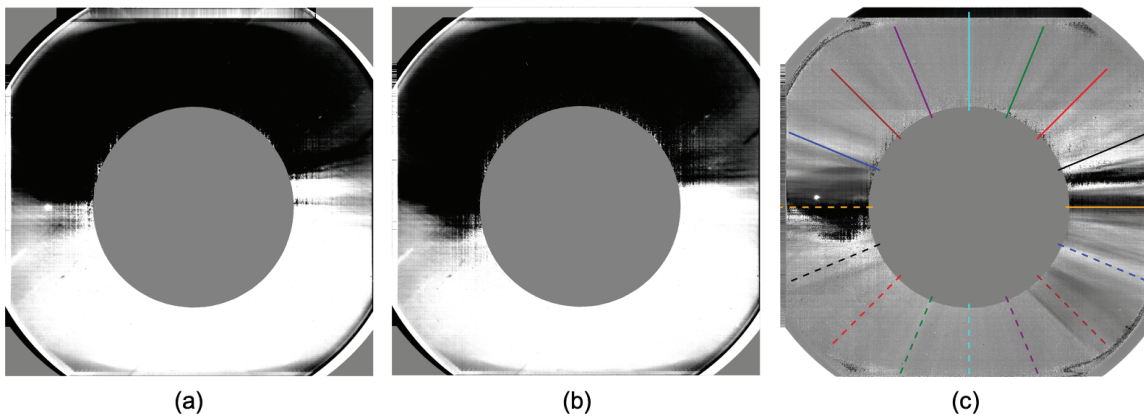


Figure 10: (a) Stray light difference map before the IO fine tuning (February 18, 2021). (b) Stray light difference map after the IO fine tuning (February 23, 2021). (c) Percent variation of post- vs pre-tuning in order to emphasize portions with high coronal change rate.

4. CONCLUSIONS

Metis is the UV and visible light coronagraph onboard Solar Orbiter. The mission is currently in its nominal phase, after a long commissioning and cruise phases during which instrument calibrations and first scientific acquisition were taken. Metis is an externally occulted coronagraph with an innovative occultation concept which is crucial in obtaining a very low stray light level (see section 1.1). In fact, no noteworthy sign of stray

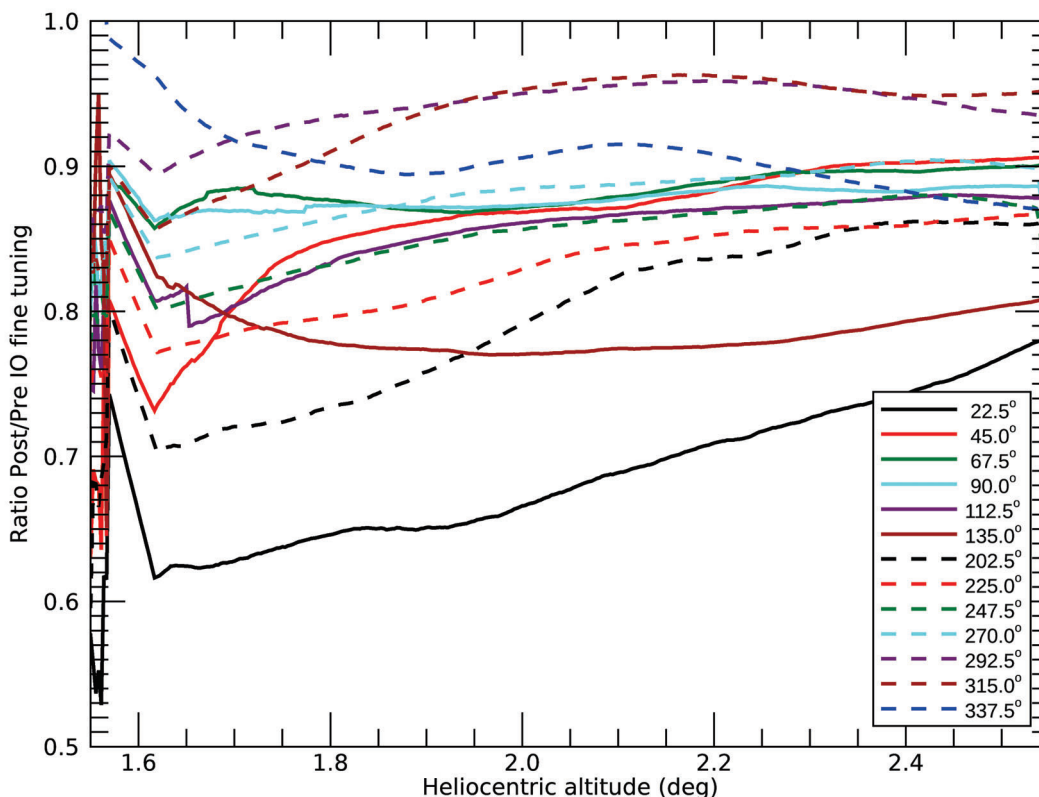


Figure 11: Ratios of the averaged radial profiles taken on stray light difference maps post- and pre- IO fine tuning.

light can be detected in Metis raw images taken at the first Solar Orbiter close-up perihelion at 0.32 UA. Such brilliant performance in stray light reduction has been obtained with a long and careful optimization process which required three successive position modifications of the internal occulter IO, the diaphragm that is conjugated to the inverted external occulter IEO with respect to the primary mirror. The IO is designed to block the light diffracted by the IEO edge and imaged by M1; it is installed on a two axis motorized stage that can be remotely controlled. A first optimization of the IO position was performed during on-ground calibrations. Launch vibrations likely induced some changes in the IO position and a further modification was then needed in flight as well (see sections 2.1 and 2.2). A first rough optimization was performed in flight with a dedicated procedure that involved a spacecraft 180° roll. Successively, a fine adjustment was also performed with the spacecraft closer to the Sun, in order to operate in worse stray light conditions (thus, close to the most challenging conditions for the coronagraph). A method has been described to evaluate the goodness of the fine adjustment over the rough one (see section 3). The results demonstrate that the fine adjustment improved the stray light reduction performance by 5% to 40% over the Metis FOV, depending on the image portion.

ACKNOWLEDGMENTS

Solar Orbiter is a space mission of international collaboration between ESA and NASA, operated by ESA. Metis was built and operated with funding from the Italian Space Agency (ASI), under contracts to the National Institute of Astrophysics (INAF) and industrial partners. Metis was built with hardware contributions from Germany (Bundesministerium für Wirtschaft und Energie through DLR), from the Czech Republic (PRODEX) and from ESA.

Metis team thanks the former PI, Ester Antonucci, for leading the development of Metis until the final delivery to ESA.

REFERENCES

- [1] Antonucci, E., Romoli, M., Andretta, V., Fineschi, S., Heinzl, P., Moses, J. D., Naletto, G., Nicolini, G., Spadaro, D., Teriaca, L., Berlicki, A., Capobianco, G., Crescenzo, G., Da Deppo, V., Focardi, M., Frassetto, F., Heerlein, K., Landini, F., Magli, E., Marco Malvezzi, A., Massone, G., Melich, R., Nicolosi, P., Noci, G., Pancrazzi, M., Pelizzo, M. G., Poletto, L., Sasso, C., Schühle, U., Solanki, S. K., Strachan, L., Susino, R., Tondello, G., Uslenghi, M., Woch, J., Abbo, L., Bemporad, A., Casti, M., Dolei, S., Grimani, C., Messerotti, M., Ricci, M., Straus, T., Telloni, D., Zuppella, P., Auchère, F., Bruno, R., Ciaravella, A., Corso, A. J., Alvarez Copano, M., Aznar Cuadrado, R., D'Amicis, R., Enge, R., Gravina, A., Jejič, S., Lamy, P., Lanzafame, A., Meierdierks, T., Papagiannaki, I., Peter, H., Fernandez Rico, G., Giday Sertsu, M., Staub, J., Tsinganos, K., Velli, M., Ventura, R., Verroi, E., Vial, J.-C., Vives, S., Volpicelli, A., Werner, S., Zerr, A., Negri, B., Castronuovo, M., Gabrielli, A., Bertacin, R., Carpentiero, R., Natalucci, S., Marliani, F., Cesa, M., Laget, P., Morea, D., Pieraccini, S., Radaelli, P., Sandri, P., Sarra, P., Cesare, S., Del Forno, F., Massa, E., Montabone, M., Mottini, S., Quattropiani, D., Schillaci, T., Boccardo, R., Brando, R., Pandi, A., Baietto, C., Bertone, R., Alvarez-Herrero, A., García Parejo, P., Cebollero, M., Amoruso, M., and Centonze, V., “Metis: the Solar Orbiter visible light and ultraviolet coronal imager,” *A&A* **642**, A10 (Oct. 2020).
- [2] Müller, D., St. Cyr, O. C., Zouganelis, I., Gilbert, H. R., Marsden, R., Nieves-Chinchilla, T., Antonucci, E., Auchère, F., Berghmans, D., Horbury, T. S., Howard, R. A., Krucker, S., Maksimovic, M., Owen, C. J., Rochus, P., Rodriguez-Pacheco, J., Romoli, M., Solanki, S. K., Bruno, R., Carlsson, M., Fludra, A., Harra, L., Hassler, D. M., Livi, S., Louarn, P., Peter, H., Schühle, U., Teriaca, L., del Toro Iniesta, J. C., Wimmer-Schweingruber, R. F., Marsch, E., Velli, M., De Groof, A., Walsh, A., and Williams, D., “The Solar Orbiter mission. Science overview,” *A&A* **642**, A1 (Oct. 2020).
- [3] Romoli, M., Antonucci, E., Andretta, V., Capuano, G. E., Da Deppo, V., De Leo, Y., Downs, C., Fineschi, S., Heinzl, P., Landini, F., Liberatore, A., Naletto, G., Nicolini, G., Pancrazzi, M., Sasso, C., Spadaro, D., Susino, R., Telloni, D., Teriaca, L., Uslenghi, M., Wang, Y. M., Bemporad, A., Capobianco, G., Casti, M., Fabi, M., Frassati, F., Frassetto, F., Giordano, S., Grimani, C., Jerse, G., Magli, E., Massone, G., Messerotti, M., Moses, D., Pelizzo, M. G., Romano, P., Schühle, U., Slemmer, A., Stangalini, M., Straus, T., Volpicelli, C. A., Zangrilli, L., Zuppella, P., Abbo, L., Auchère, F., Aznar Cuadrado, R., Berlicki, A., Bruno, R., Ciaravella, A., D'Amicis, R., Lamy, P., Lanzafame, A., Malvezzi, A. M., Nicolosi, P., Nisticò, G., Peter, H., Plainaki, C., Poletto, L., Reale, F., Solanki, S. K., Strachan, L., Tondello, G., Tsinganos, K., Velli, M., Ventura, R., Vial, J. C., Woch, J., and Zimbardo, G., “First light observations of the solar wind in the outer corona with the Metis coronagraph,” *A&A* **656**, A32 (Dec. 2021).
- [4] Romoli, M., “First data and instrument performance from Metis coronagraph on Solar Orbiter,” in [*AGU Fall Meeting Abstracts*], **2020**, SH038–04 (Dec. 2020).
- [5] Fineschi, S., Naletto, G., Romoli, M., Da Deppo, V., Antonucci, E., Moses, D., Malvezzi, A. M., Nicolini, G., Spadaro, D., Teriaca, L., Andretta, V., Capobianco, G., Crescenzo, G., Focardi, M., Frassetto, F., Landini, F., Massone, G., Melich, R., Nicolosi, P., Pancrazzi, M., Pelizzo, M. G., Poletto, L., Schühle, U., Uslenghi, M., Vives, S., Solanki, S. K., Heinzl, P., Berlicki, A., Cesare, S., Morea, D., Mottini, S., Sandri, P., Alvarez-Herrero, A., and Castronuovo, M., “Optical design of the multi-wavelength imaging coronagraph Metis for the solar orbiter mission,” *Experimental Astronomy* **49**, 239–263 (May 2020).
- [6] Landini, F., Romoli, M., Capobianco, G., Vives, S., Fineschi, S., Massone, G., Loreggia, D., Turchi, E., Guillon, C., Escolle, C., Pancrazzi, M., and Focardi, M., “Improved stray light suppression performance for the solar orbiter/METIS inverted external occulter,” in [*Solar Physics and Space Weather Instrumentation*

- V], Fineschi, S. and Fennelly, J., eds., *Society of Photo-Optical Instrumentation Engineers (SPIE) Conference Series* **8862**, 886204 (Sept. 2013).
- [7] Landini, F., Romoli, M., Vives, S., Baccani, C., Escolle, C., Pancrazzi, M., Focardi, M., Da Deppo, V., Moses, J. D., and Fineschi, S., “Coating and surface finishing definition for the Solar Orbiter/METIS inverted external occulter,” in [*Advances in Optical and Mechanical Technologies for Telescopes and Instrumentation*], Navarro, R., Cunningham, C. R., and Barto, A. A., eds., *Society of Photo-Optical Instrumentation Engineers (SPIE) Conference Series* **9151**, 91515H (July 2014).